scientific reports

Check for updates

OPEN

Light-emitting diode red light attenuates epidermal thickening and keratinocyte proliferation in psoriasis models

Evan Austin[1,2,4], Eugene Koo[3], Margaret Kabakova[1,2], Marc Cohen[1,2], Alana Kurtti[1,2], Andrew Mamalis[1,5], Emanuel Maverakis[3], Roslyn Rivkah Isseroff[3,4] & Jared Jagdeo[1,2,3,4,6]✉

Psoriasis is an immune-mediated skin condition that impacts approximately 3% of the United States population, with limited adjunctive therapy options. This study investigates the effects of light emitting diode red light (LED-RL) as a potential adjunct. Using in vitro keratinocytes, three-dimensional (3D) recapitulated skin models, and a mouse model, LED-RL's impact on keratinocyte proliferation and epidermal thickness was assessed. Our findings show that LED-RL significantly reduced keratinocyte proliferation without inducing apoptosis, likely through cell cycle modulation and decreased phosphorylation of STAT3, a pathway critical to psoriasis pathogenesis. In the 3D skin models, LED-RL at a dose of 640 J/cm^2 reduced epidermal thickness in IL-22-stimulated samples. In mouse models, a daily dose of 1280 J/cm^2 decreased epidermal thickness when co-administered and administered following the development of a psoriasiform phenotype with imiquimod. These results suggest LED-RL may offer an efficacious and cost-effective alternative to existing therapies for mild to moderate psoriasis.

Psoriasis is a chronic, immune-mediated skin condition impacting approximately 3% of the U.S. population[1]. The estimated health burden of psoriasis in 2013 was $35.2 billion[2]. Patients experience functional and aesthetic impairments, often leading to an overall decreased quality of life[3]. Immune cells such as Th17, Th22, and Th1 contribute to pathogenesis by releasing IL-17a, IL-22, IFNγ, and TNF, which stimulate keratinocytes and the proliferation characteristic of psoriasis[4]. Treatment options include topicals, phototherapy, oral immunosuppressants, and biologics. For moderate to severe psoriasis, narrow-band ultraviolet-B (UV-B) is a part of the standard of care. Limitations of UV-B phototherapy include the risk of photoaging, hyperpigmentation, and barriers to care, such as transportation and the continued low accessibility in home settings due to cost and reimbursement[5–7]. Red light (RL; 633 +/- 15 nm) phototherapy for psoriasis may represent a cost-effective, accessible, and safer alternative.

The skin is recognized not merely as a physical barrier but also as an active neuro-immuno-endocrine organ that senses and integrates various environmental signals, including electromagnetic radiation. Different wavelengths of solar and artificial light have distinct biological effects mediated through specific photoreceptors and neural pathways within the skin[8–10]. This broader understanding underscores the importance of elucidating the specific cellular and molecular interactions engaged by RL, positioning our investigation within the emerging paradigm of photo-neuro-immuno-endocrinology.

Previous research has evaluated the potential for visible light phototherapy to treat psoriasis[11,12]. Blue light (BL) decreased keratinocyte proliferation, possibly via a ROS-mediated mechanism[13,14]. However, there is limited research to determine if RL monotherapy can treat psoriasis. Previous studies combine RL with other wavelengths, including near-infrared light[15,16]. RL is therapeutically advantageous because it allows a greater number of photons to reach a deeper penetration than BL. RL has also been more closely linked to mitochondrial photobiomodulation mechanisms[17].

[1]Dermatology Service, Veterans Affairs New York Harbor Healthcare System - Brooklyn Campus, Brooklyn, NY, USA. [2]Department of Dermatology, State University of New York, Downstate Health Sciences University, Brooklyn, NY, USA. [3]Department of Dermatology, University of California at Davis, Sacramento, CA, USA. [4]Dermatology Service, Sacramento VA Medical Center, Mather, CA, USA. [5]Department of Dermatology, Modesto Medical Center, Modesto, CA, USA. [6]Department of Dermatology, SUNY Downstate Medical Center, 450 Clarkson Avenue, 8th Floor, Brooklyn, NY 11203, USA. ✉email: jrjagdeo@gmail.com

Our lab previously characterized the effect of high fluence RL from light-emitting diodes (LED-RL) on normal human dermal fibroblasts and melanoma cells[18,19]. LED-RL differs from RL lasers (e.g., PDL and ruby laser) as LED treats a field of skin similar to NB-UVB. Previous research by our group demonstrates that LED-RL significantly inhibits fibroblast and melanoma proliferation[18,20]. Herein, this research aims to characterize the effects of RL using in vitro, three-dimensional (3D) recapitulated, and mouse models of psoriasis. Herein, LED-RL had an inhibitory effect on human keratinocyte proliferation and decreased epidermal thickness in 3D skin models and mice. Our results demonstrate the potential for LED-RL to be used as a novel alternative treatment modality for psoriasis phototherapy.

Results

LED-RL inhibits keratinocyte proliferation through a non-apoptotic pathway

To determine whether LED-RL inhibits keratinocyte proliferation, HaCaTs cells were irradiated with 320 and 640 J/cm^2 LED-RL, and their cell counts were measured at 24 and 48 h post irradiation. There was a statistically significant dose-dependent decrease in cell count 48 h after LED-RL treatment (Fig. 1A). This experiment was repeated in primary keratinocytes and resulted in a similar inhibition of proliferation 48 h after LED-RL treatment (Fig. 1B and C). The keratinocytes had no gross morphological changes after the LED-RL treatment (Fig. 1C). Keratinocytes were stimulated with IL-22 to induce a hyperproliferative phenotype (Fig. 1D)[21,22]. IL-22 is a known keratinocyte proliferative cytokine[21,22]. LED-RL attenuated IL-22 mediated increases in keratinocyte proliferation (Fig. 1D), demonstrating efficacy in an in vitro psoriasiform phenotype.

There was no difference in apoptosis between keratinocyte samples treated with LED-RL and control samples at 0, 12, and 24 h after treatment as assessed by Annexin-V flow cytometry (Fig. 2A- B). Similarly, there was no difference in pro-apoptotic cleaved caspase 3 in the LED-RL treated group compared to control (Supplemental Fig. 1). Since LED-RL did not induce cell apoptosis, cell cycle analysis by flow cytometry was employed to determine if LED-RL affected cell cycles. Twenty-four hours after 640 J/cm^2 LED-RL treatment, there was a decrease in the portion of cells in the S-phase (6.18%) and an increase in G1-phase cells (6.98%) (Fig. 2C). At 48 h, the percentage of 640 J/cm^2 LED-RL treated cells in the S-phase of the cell cycle was decreased compared to the control (3.57%), and the number of cells in the G1-phase was greater (4.89%), but the difference was not statistically significant (Fig. 2C). We previously demonstrated that the RL duration of effect is approximately 18 h in human dermal fibroblasts[23]. Phosphorylation of STAT3 is upregulated in psoriatic keratinocytes[24]. LED-RL decreased phosphorylation of STAT3 in IL-22 stimulated cells when compared to control samples 24 h after treatment (Fig. 2D and Supplemental Fig. 2). There was no difference in K17 expression after LED-RL (Supplemental Fig. 3).

RL reduces epidermal thickness in 3D and murine skin models

A 3D epidermis model was treated with IL-22 and LED-RL for 9 days to determine if LED-RL could inhibit IL-22 induced proliferation in this model. There was a statistically significant reduction in epidermal thickness in H&E-stained IL-22 stimulated LED-RL-treated samples compared to control samples. (Fig. 3A-B). There was no statistically significant difference in proliferative (Ki-67) and psoriasis markers (involucrin) signals between all treated samples (Supplemental Fig. 3–4).

Next, LED-RL efficacy was assessed using a BALB/c imiquimod model of psoriasis. Two different protocols were utilized. In the treatment protocol, mice (n = 6) received 4 days of imiquimod followed by 4 days of LED-RL. Daily administration of 1280 J/cm^2 and twice daily administration of 640 J/cm^2 were compared to a single control using Dunnett's multiple comparison (Fig. 4). Both 1280 J/cm^2 and twice daily administration of 640 J/cm^2 reduced epidermal thickness compared to control, but only 1280 J/cm^2 achieved significance (1280 J/cm^2 LED-RL: 39.46 µm vs. control: 51.51 µm, p = 0.044; 640 J/cm^2 LED-RL: 43.35 µm vs. control: 51.51 µm, p = 0.250). In the prevention protocol, mice (n = 6) were concurrently treated with 4 days of imiquimod and 1280 J/cm^2 daily LED-RL based on preliminary relative efficacies in previous protocols (Fig. 5)[20]. In the prevention protocol, 1280 J/cm^2 irradiation daily LED-RL significantly reduced epidermal thickness (control: 89.36 µm vs. RL: 71.63 µm, p = 0.011).[20] A vehicle control experiment (white petrolatum without imiquimod) was performed, and neither daily 1280 J/cm^2 (18.49 µM, n = 2) nor twice daily 640 J/cm^2 (16.37 µM, n = 2) appeared to change epidermal thickness compared to the control (17.48 µM, n = 2)(Supplemental Fig. 5). Statistics were not performed in the vehicle control experiment. The LED-RL protocols were well tolerated in imiquimod and vehicle mice. The epidermis of mice in the treatment and prevention protocol was examined for dyskeratotic keratinocytes ("sunburn cells") as markers of apoptosis/necrosis. There was negligible dyskeratosis in the epidermis of either the control or LED-RL treated mice in both protocols (Data not shown).

Discussion

RL-LED inhibited psoriasiform features in cell culture, 3D recapitulated skin, and murine imiquimod models. In vitro, LED-RL at fluences of 320 and 640 J/cm^2 significantly decreased keratinocyte proliferation without inducing cell death or apoptosis. Keratinocytes were then stimulated with IL-22 to produce a psoriasiform phenotype. In the IL-22 stimulated keratinocytes, 640 J/cm^2 LED-RL was also able to decrease cell proliferation. Given that RL-LED did not induce apoptosis, we performed cell cycle analysis to determine whether LED-RL alters keratinocyte proliferation via modulation of the cell cycle. At 24 h following 640 J/cm^2 LED-RL treatment, there was a decrease in the proportion of keratinocytes in the S-phase and an increase in cells in the G1-phase. This trend persisted at 48 h, suggesting a shift toward G1 arrest, though the changes were not statistically significant. These findings support the hypothesis that RL-LED may attenuate proliferation by impeding S-phase entry, providing further mechanistic insight into its anti-proliferative effects. STAT3 phosphorylation was decreased in keratinocyte treated with LED-RL[25]. STAT3 facilitates the activation of distinct gene sets across

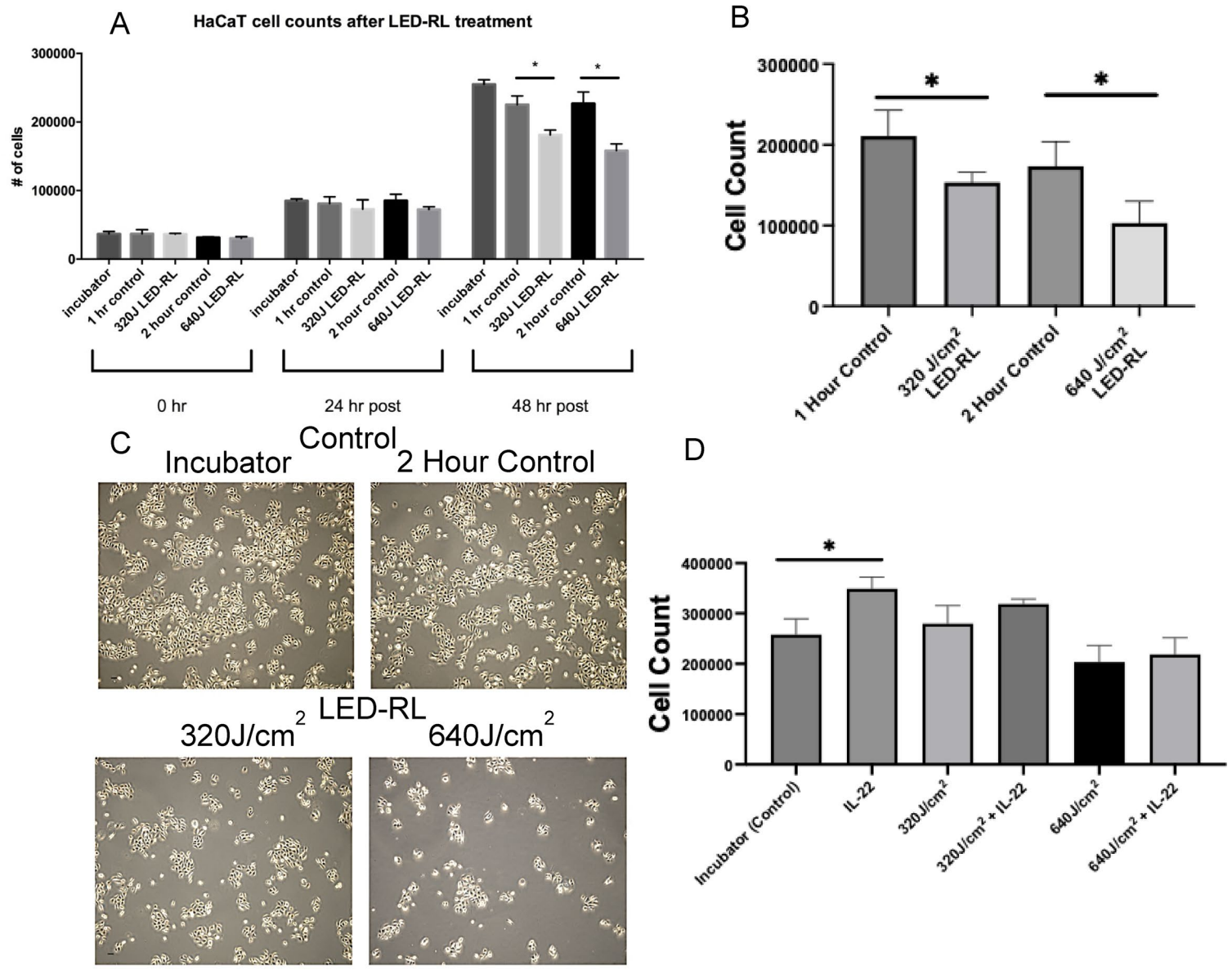

Fig. 1. LED-RL inhibits keratinocyte proliferation. (**A**) Total cell counts in control and LED-RL treated HaCaTs ($n = 3$ technical repeats). The incubator (negative) control remained in the 37 °C humidified incubator with 5% CO_2 throughout the treatment protocol. LED-RL and matched control treatment protocols were performed outside of the incubator. (**B**) Total cell counts of LED-RL treated human primary keratinocytes ($n = 5$ technical repeats). (**C**) Representative phase contrast images of primary keratinocytes 48 h after LED-RL treatment. (**D**) Total cell counts of primary keratinocytes pre- or untreated with IL-22 and treated with LED-RL at doses of 320 and 640 J/cm^2 ($n = 3$ technical repeats). Student's t-test was utilized to determine statistical significance between LED-RL samples and their respective temperature-matched control group (1 h to 320 J/cm^2 LED-RL; 2 hours to 640 J/cm^2 LED-RL). * denotes $p < 0.05$.

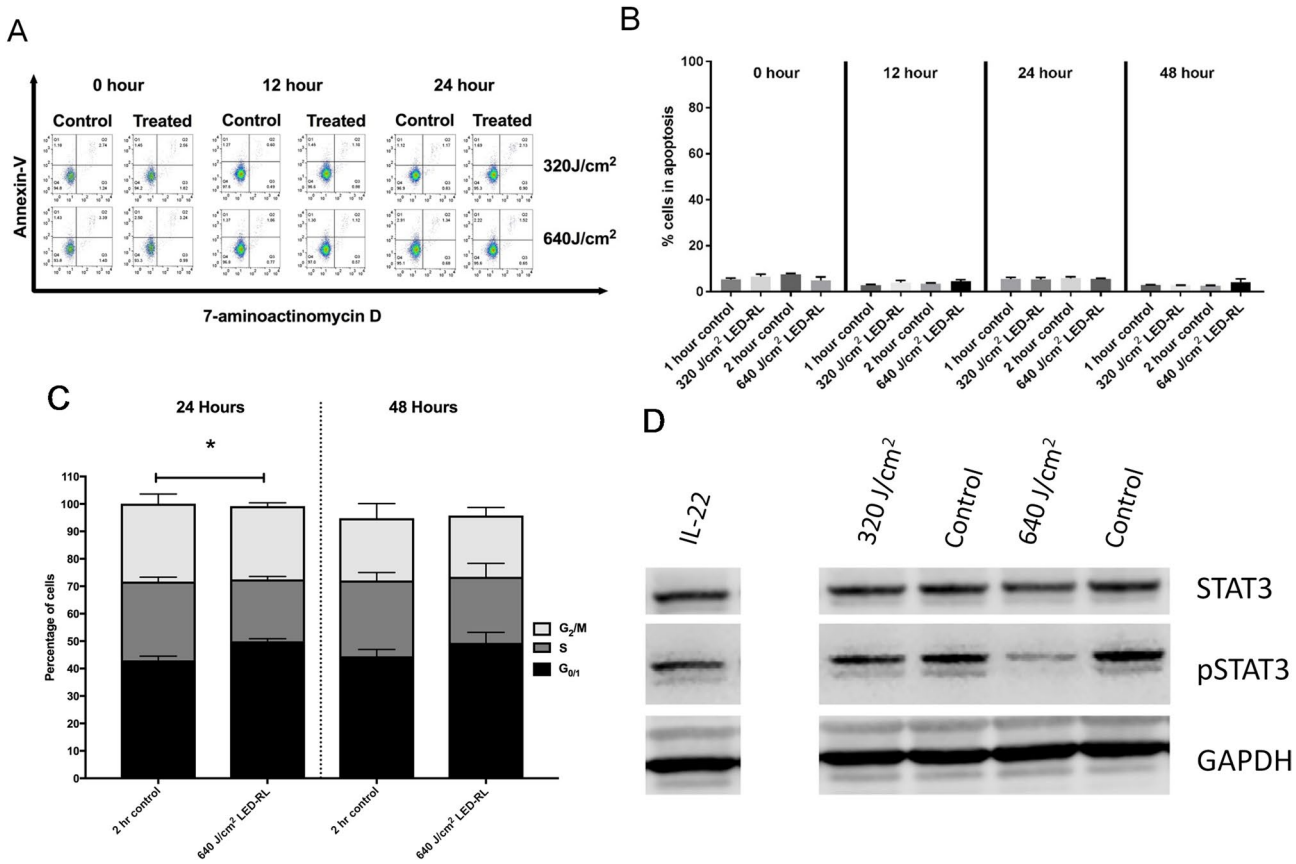

Fig. 2. LED-RL does not increase cell apoptosis but decreases the S-phase of the cell cycle and STAT3 phosphorylation. (**A**) Representative scatterplot of flow cytometry diagrams of LED-RL treated primary keratinocyte samples at 0, 12, and 24 h after treatment. The y-axis represents annexin-V, and the x-axis represents 7-aminoactinomycin D (7-AAD). (**B**) Total cell apoptotic percentage in LED-RL treated cells ($n = 3$ technical repeats). (**C**) Cell cycle diagram using propidium iodide flow cytometry ($n = 4$ technical repeats). (**D**) Western blot of pSTAT phosphorylation of IL-22 pre-treatment followed by LED-RL or control treatment. Lane 1 demonstrates IL-22 positive control. Gel images were cropped from different parts of the same gel and converted to black & white as fluorescent probes were used. Non-cropped images are available in the supplement ($n = 3$ technical repeats). Student's t-test was utilized to determine statistical significance between LED-RL samples and their respective temperature-matched control group. * denotes $p < 0.05$.

various cell types, including inflammatory and proliferative pathways[25,26]. In transgenic mouse models, direct overexpression of STAT3 in keratinocytes produced a psoriatic phenotype[24]. Future experiments would be needed to quantify STAT3 expression in vivo.

Emerging evidence indicates that the skin functions as a neuro-immuno-endocrine organ, integrating external signals such as ultraviolet (UV) and visible light radiation to modulate systemic and local homeostasis through neuroendocrine and immune signaling pathways. Recent reviews have highlighted the concept of photo-neuro-immuno-endocrinology, describing how electromagnetic radiation engages cutaneous receptors and initiates cascades involving neuropeptides, neurotransmitters, and immune mediators[9,10]. Although our study primarily demonstrates the direct effects of RL on keratinocyte proliferation and epidermal thickness, it is plausible that RL could also modulate cutaneous neuroimmune signaling pathways. Future studies investigating potential neuroendocrine mechanisms, including assessment of neuropeptide levels and neural activation markers, could provide valuable insights into the broader implications of LED-RL therapy.

LED-RL experimental protocols were translated to 3D and murine models. In the 3D skin model, LED-RL decreased epidermal thickness when the keratinocytes were stimulated with IL-22. In the imiquimod mouse model, fluences of 1280 J/cm^2 similarly decreased epidermal skin thickness when assessed using H&E staining. LED-RL was well tolerated in the mouse model and did not change the epidermal thickness of non-psoriatic vehicle mice. Twice daily 640 J/cm^2 did not significantly decrease epidermal thickness, but this finding was likely related to insufficient statistical power and could be investigated in future studies. Combination phototherapy for the application of psoriasis with LED and laser diodes may be an alternative approach to achieve higher fluences and decreased total treatment time. LED-RL does not induce direct DNA damage via pyrimidine dimers or 6 – 4 photoproducts[27]. In previous clinical protocols, fluences of 480 J/cm2 and 640 J/cm^2 caused blistering when the LED-RL array was placed directly on human skin[28]. However, the mice were placed in air-conditioned treatment

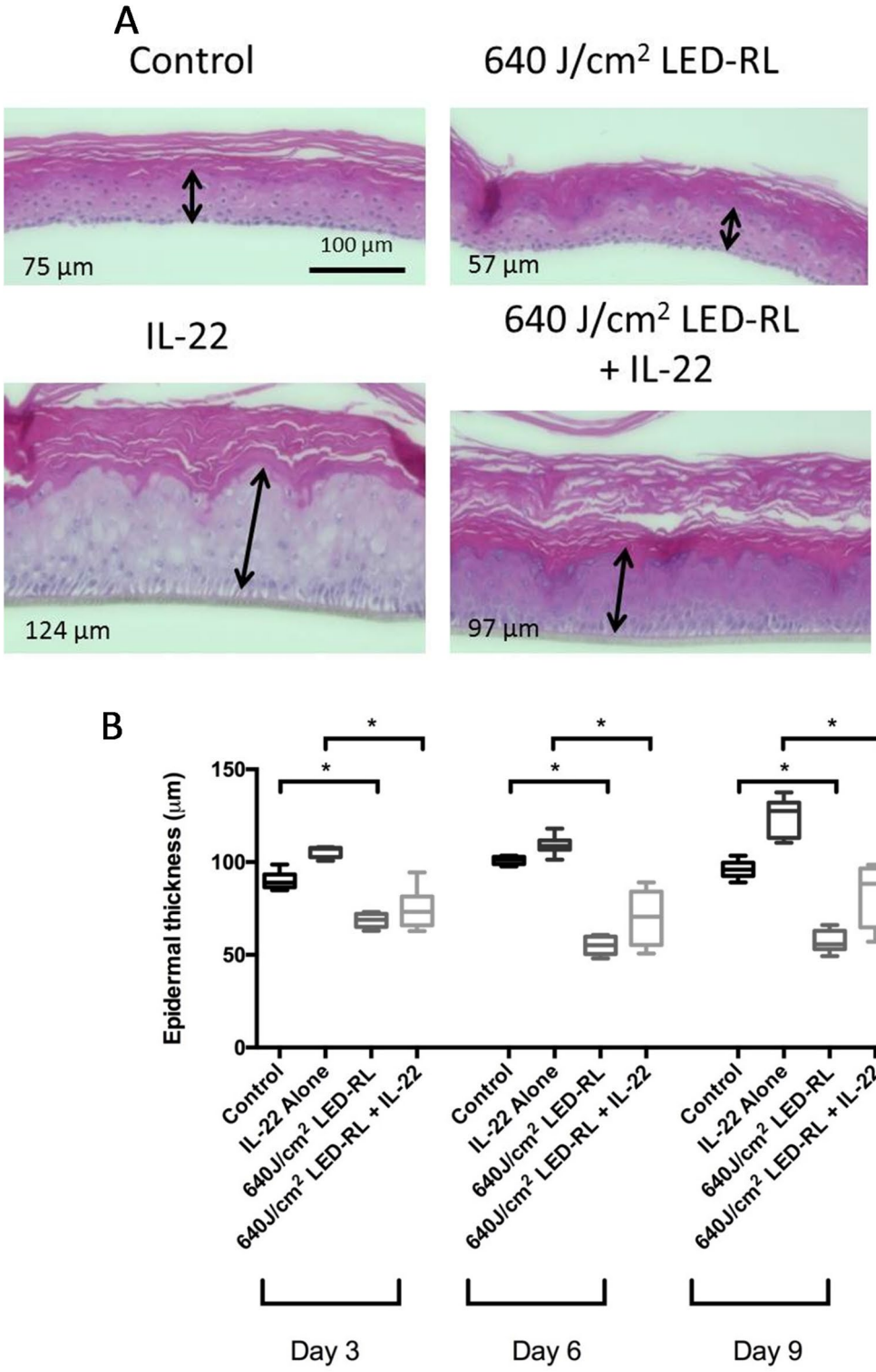

Fig. 3. Skin equivalents stimulated with IL-22 have a thickened epidermis and are reduced by LED-RL. (**A**) Epidermal thickness in IL-22 stimulated and LED-RL treated human 3-dimensional (3D) epidermal skin models. (**B**) Relative epidermal thickness ($n = 8$ technical repeat). The experiment was repeated 4 times. ANOVA was utilized to determine statistical significance between all the groups.

cages. Therefore, temperature regulation is important when designing protocols using high fluences of visible light.

Our findings complement and extend previous research in phototherapy for psoriasis. Prior studies have demonstrated that blue light inhibits keratinocyte proliferation via ROS-mediated mechanisms, yet has a lower

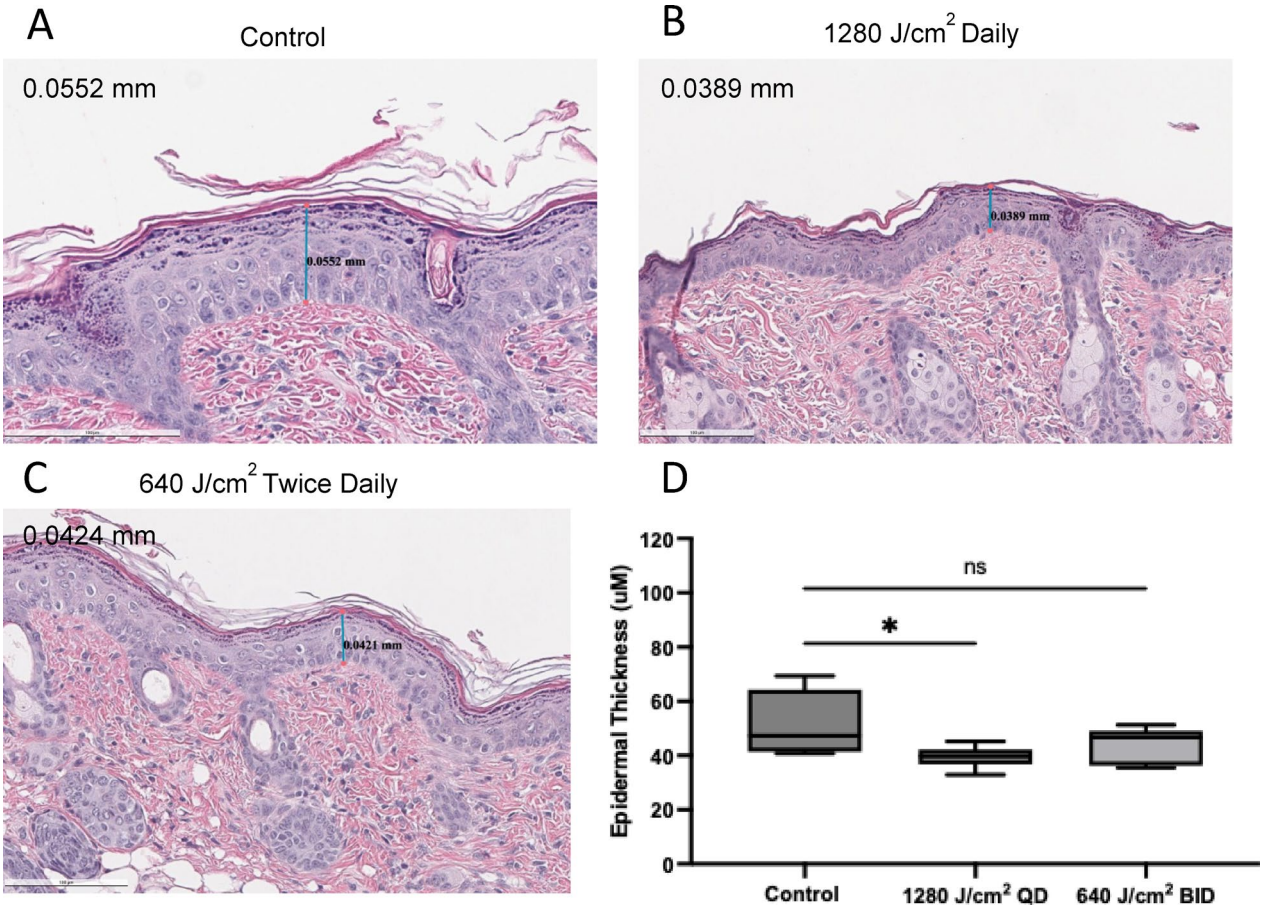

Fig. 4. Mice concurrently treated with imiquimod and LED-RL have decreased epidermal thickness compared to mice only treated with imiquimod. Topical imiquimod was applied on days 1–4. Mice were irradiated on days 1–4. Representative images of (**A**) Control, (**B**) 1280 J/cm^2 RL daily, and (**C**) 640 J/cm^2 RL twice daily groups. (**D**) Quantified epidermal thickness of control, 1280 J/cm^2 RL daily, and 640 J/cm^2 RL twice daily treatment groups ($n = 6$ technical repeats). ANOVA followed by Dunnett's multiple comparison test was used to assess significance across three groups. * denotes A p-value < 0.05.

depth of penetration compared to RL, restricting its efficacy in hyperplastic psoriatic lesions (> 2 mm thickness)[14]. RL, however, penetrates the full epidermal layer, reaching hyperproliferative keratinocytes in psoriatic plaques more effectively than BL. Previous RL studies combined wavelengths, obscuring specific RL effects[15,16]. Our study uniquely establishes the monotherapy efficacy of RL at defined fluences and wavelengths, providing clear mechanistic insights into RL-mediated effects and improvements in cellular and murine models of psoriasis.

Our study on RL-LED as a psoriasis treatment has several notable strengths and limitations. A key strength is the use of multiple experimental models, including in vitro, an in vivo murine model, and 3D recapitulated skin protocols, which enhance result validity and robustness. Additionally, our use of a commercially available LED-RL array ensures greater generalizability and reproducibility. However, there are limitations to consider. We did not directly measure immune activity. Additionally, the imiquimod model, commonly used to replicate a psoriatic phenotype, requires continuous application to maintain epidermal thickness and psoriatic features. However, mice tolerate imiquimod application for only approximately seven days due to systemic adverse events, limiting the ability to assess long-term treatment effects. Additionally, we did not directly collect or analyze circulating immune cells, which may be involved in systemic or lesional responses to RL-LED therapy. Future studies may benefit from incorporating immune cell analysis to understand the broader immunomodulatory effects of LED-RL better. While our findings provide initial evidence supporting LED-RL's efficacy in reducing keratinocyte proliferation and epidermal thickening in psoriasis models, further studies are necessary to confirm the clinical relevance of these results. Future research should investigate broader immunological effects, extended treatment durations, and larger cohorts to fully establish LED-RL as a viable therapeutic option.

Despite remarkable advancements in psoriasis treatments, including biologics, complete skin clearance remains unattainable for many patients, highlighting the ongoing need for adjunctive therapeutic options. Additionally, certain patient populations cannot tolerate biologics due to contraindications, adverse effects, or cost considerations. Our research provides a compelling scientific foundation for the potential use of RL phototherapy for psoriasis by demonstrating the effectiveness of RL to significantly decrease hallmark pathognomonic features such as epidermal thickening and keratinocyte proliferation. In contrast to topical

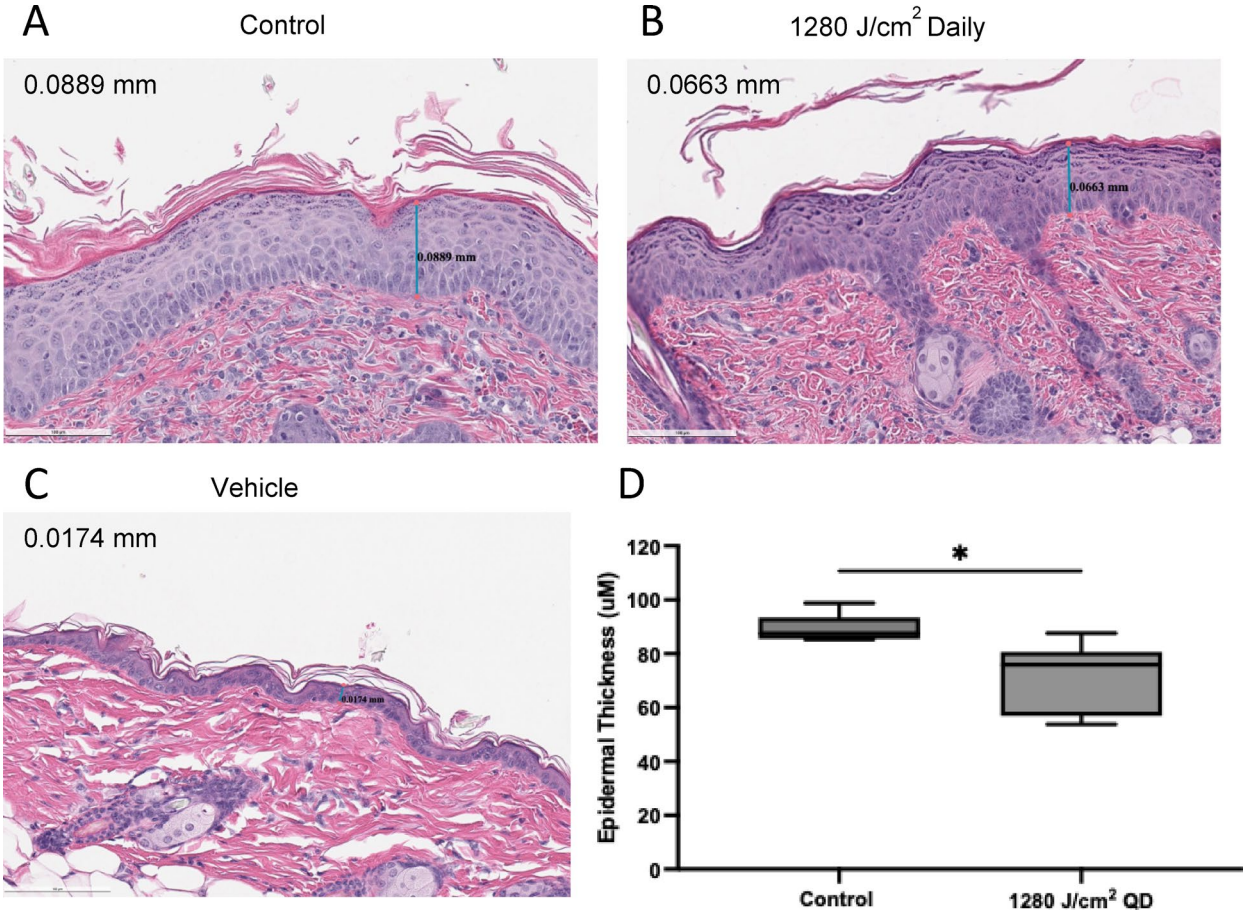

Fig. 5. 1280 J/cm^2 LED-RL daily reduced epidermal thickness in mice treated with topical imiquimod followed by LED-RL. Topical imiquimod was applied on days 1–4. LED-RL was administered on days 5–8. Representative images of (**A**) Control, (**B**) 1280 J/cm^2 RL daily groups. (**C**) Representative image of vehicle control mouse skin without imiquimod or RL treatment ($n = 2$). White petrolatum was administered on days 1–4. (**D**) Quantified epidermal thickness of control and 1280 J/cm^2 RL daily treatment groups ($n = 6$). A T-test quantified the significance between control and LED-RL. * denotes A p-value < 0.05.

and systemic treatments, LED-RL is notably safer, well-tolerated, and highly accessible. Given the considerable patient burden and limitations of existing therapies, our findings strongly support further clinical investigations to optimize RL treatment regimens and explore its integration into combination therapeutic strategies. Advancing this research could substantially enhance clinical outcomes and quality of life for psoriasis patients, addressing a critical unmet medical need.

Materials and methods

Cell culture

HaCaT keratinocytes were sub-cultured in Dulbecco's Modified Eagle Medium (Invitrogen) supplemented with 10% Fetal Bovine Serum (Atlanta Biologicals) and 1% Antibiotic-Antimycotic (Invitrogen). Primary keratinocytes were isolated from the neonatal foreskin using a University of California, Davis Institutional Review Board-approved protocol. As part of the tissue donation protocol, informed consent was obtained from a parent and/or legal guardian. All protocols were followed according to the relevant guidelines. Primary keratinocytes were sub-cultured in Basal Cell Medium supplemented with Keratinocyte Growth Kit (ATCC). Primary keratinocytes from passages 3 or 4 were used for all experiments. Multiple tissue donors were utilized throughout the protocols. Each experimental run utilized HaCaT or keratinocytes from a single donor. Experiments protocols were repeated with keratinocytes of different lineages to confirm results with biological variability. IL-22 (R&D Systems) was supplemented to Basal Cell Medium at 30 ng/ml 24 h after passage, before experiments. All cultures were maintained in a 37° C humidified incubator with 5% CO_2.

LED array specifications

The LED light source used for all in vitro and 3D skin model experiments was commercially available Omnilux new-U handheld units (PhotoTherapeutics) as previously described (15). Briefly, the LED array consists of a 4.7 × 6.1 cm rectangular aperture and emits light at a wavelength of 633 ± 30 nm with a power density of 872.6 W/m2 at room temperature when placed at a distance of 10 mm from the bottom of the tissue culture

dish to the LED array. The LED light source used for the mice studies was commercially available Omnilux Revive 2 (GlobalMed Technologies) as previously described[20]. Briefly, the LED-RL array consists of a 35 × 32 cm rectangular panel and emits light at a wavelength of 633 ± 15 nm with a power density of 87 mW/cm^2 at room temperature when measured at the light array surface.

Keratinocyte irradiation

LED-RL protocols were performed as previously described[20,29]. LED-RL irradiations were performed outside of the incubator. LED-RL treated keratinocytes were temperature-matched to control groups outside of the incubator (1 h to 320 J/cm^2 LED-RL; 2 hours to 640 J/cm^2 LED-RL) for statistics. Keratinocytes were irradiated at a distance of 10 mm from the bottom of the tissue culture dish to the LED array. LED arrays were turned on 15 min before irradiation treatments to warm the surface under the array. This allowed optimal temperature regulation of keratinocyte cultures underneath the LED arrays, measured at 33–34 °C by a thermal probe (Grainger) throughout the entire irradiation period. Temperature-matched control keratinocytes were placed on EchoTherm chilling/heating dry bath plates (Torrey Pines Scientific) set to 34 °C and protected from light. The temperature of keratinocyte cultures on these digital warming plates was also measured to be between 33 and 35 °C by thermal probe. An incubator (negative) control remained in the 37 °C humidified incubator with 5% CO_2 throughout the treatment protocols and served as an internal reference. After irradiation, culture dishes were returned to the incubator until further processing for assays at their appropriate time.

Cell counting assay

To assess LED-RL effects on keratinocyte proliferation, HaCaT and primary keratinocyte cultures were irradiated with previously determined doses of LED-RL and counted 48 h after the initial irradiation, as previously described ([20]). Briefly, counted cells were obtained from the culture medium supernatant, wash supernatant, and trypsin-mediated cell lifting. Cell counts were calculated by obtaining the product of the final sample suspension volume measured with a pipette and the cell concentration of the sample as determined by a hemacytometer and trypan blue.

In vitro microscopy

Images of cell cultures after LED-RL treatment and histological slides were made with 10x scans using the BZ-9000 (Keyence). The epidermal thickness of H&E-stained histological slides was analyzed using the software provided with the BZ-9000 (Keyence).

Apoptosis assay

To assess any changes in the percentage of cells undergoing apoptosis after LED-RL treatment, the FlowCollect Annexin Red Kit (Millipore) was used, and the manufacturer's protocol was followed. Briefly, after keratinocytes were treated with LED-RL, the cells were detached from culture plates with 0.025% trypsin-EDTA and collected in 5 ml polystyrene flow tubes (Corning). Cells were centrifuged, supernatant discarded, and resuspended in 200 µL of Annexin-V Buffer containing a 1:40 dilution of Annexin-V. Annexin-V was incubated for 15 min at 37 °C, then 5 µl of 7-aminoactinomycin D (7-AAD) was added. Cells were immediately analyzed by flow cytometry on FACSCalibur (BecktonDicson, USA).

Cell cycle assay

Changes in the cell cycle were assessed with propidium iodide flow cytometry analysis. Keratinocytes were collected and fixed with 4% formaldehyde for 10 min at 4 °C. After washing with chilled PBS, cells were suspended in PBS with 0.1% Triton X-100. Cells were incubated with PI (50ug/ml) and RNAase A (10 ug/ml) after PBS washing. Cells were analyzed with flow cytometry. The percentage of cells in G0/1, S, and G2/M phases of the cell cycle was calculated. Flow cytometry will be performed using a Guava cytometer (Millipore Sigma). FlowJo software was used to gate and analyze flow cytometric results.

Western blot

To determine changes in the protein content of keratinocytes, previously described protocols for Western blot were used[18]. Briefly, protein was isolated using Cell Lysis Buffer supplemented with phenylmethylsulfonyl fluoride and Protease/phosphatase Inhibitor Cocktail (Cell Signaling Technology). Protein concentration was assessed using Bradford reagent (BioRad) and read on a microplate reader (Biotek) at 595 nm wavelength. 20 µg protein samples were prepared with LDS sample buffer and reducing agent (Invitrogen) and placed into individual wells of 8–12% Tris-Bis gradient cast gels (Novex). After gel electrophoresis, the protein was transferred to an Immobilon PVDF membrane (Millipore). After the transfer, the membrane was blocked with TBS-based Odyssey blocking buffer (LiCor) for 1 h. Primary antibodies against STAT3, phospho-STAT3, Caspase 3, cleaved Caspase 3, Keratin 17 (Cell Signaling Technology), and GAPDH (Millipore) were diluted in Odyssey blocking buffer with 0.1% Tween-20 at 1:1000 for STAT3, phospho-STAT3, Caspase 3, cleaved Caspase 3, Keratin 17, and 1:5000 for GAPDH. Blocking buffer was decanted, and membranes were incubated with primary antibodies at 4 °C overnight on an agitator. Primary antibody was decanted, and membranes were washed three times in TBS with 0.1% Tween-20. After the last wash, membranes were incubated with donkey anti-mouse or rabbit IR-dye secondary antibodies (LiCor) diluted to 1:5000 in TBS Odyssey blocking buffer with 0.1% Tween-20 and 0.1% SDS for 1 h at room temperature. Secondary antibody was decanted, and membranes were washed three times in TBS with 0.1% Tween-20 and a final wash of TBS alone. Membranes were imaged on Odyssey FC (LiCor), and fluorescence intensity values were used to measure signal strength. Signal for pSTAT3 was normalized to STAT3. Signal for K17, cleaved caspase 3, and caspase 3 were semi-qualitatively assessed.

3D reconstituted human epidermis and histology

EpiDerm-200 3D skin constructs (MatTek Corporation) were grown and maintained in EPI-100-NMM medium and cultured as suggested by the manufacturer. Briefly, the skin constructs were placed on culture stands within 6-well plates to grow epidermis at the air-liquid interface. Upon arrival, skin constructs were acclimated for 24 h in a 37 °C humidified incubator. After the acclimation period, the epidermal culture medium was changed, and 30 ng/ml IL-22 was added to the stimulated samples. Medium was changed every other day, and stimulated samples continued to receive 30 ng/ml IL-22. To irradiate treatment samples with 640 J/cm^2 LED-RL, epidermal culture wells were transferred to a 35 mm culture dish with EPI-100-NMM medium. After treatment, epidermal culture wells were transferred back to 6-well plates and placed back into a 37 °C humidified incubator. After 3, 6, and 9 days of treatments and stimulation, skin constructs were washed with PBS three times and fixed in 4% paraformaldehyde for 4 h. After fixation, skin constructs were washed with PBS three times and processed for paraffin embedding to perform subsequent histological examination. Experiment was repeated 4 times with similar trends.

Mouse care and use

BALB/C mice (The Jackson Laboratory) were housed and cared for in the animal facility in the Department of Comparative Medicine at SUNY Downstate. The protocols were approved by the SUNY Downstate Institutional Animal Care and Use Committee (Protocol ID: 19-10564). Experiments were performed following institutional guidelines and regulations. Animals were provided a standard chow diet and always had full access to food and water. Animals were humanely treated, monitored, and euthanized after our study. All methods are reported following ARRIVE guidelines (https://arriveguidelines.org).

Adult mouse euthanasia protocol

At the study endpoint, following humane endpoints, the mice were euthanized. Mice were placed in a transparent chamber for continual observation, and inhaled carbon dioxide was delivered at a 10–30% fill rate until respirations ceased. Euthanasia was confirmed using cervical dislocation.

Imiquimod application

Topical imiquimod (5% in petrolatum) or vehicle was applied to the shaved backs of mice once daily for 4 days[20]. Topical imiquimod has been previously demonstrated to increase epidermal thickness and mimic the pathological features of psoriasis.

Treatment protocol

For the treatment protocol, mice ($n=6$) were treated with once-daily topical imiquimod or petrolatum vehicle on days 1–4. On days 5–8, the mice received either 1280 J/cm^2 RL once daily (QD) or 4 days of 640 J/cm^2 twice-daily (BID). On day 9, the mice were sacrificed, and tissue samples were collected for pathological analysis.

Prevention protocol

For the prevention protocol, mice ($n=6$) were treated with once-daily topical imiquimod on days 1–4. After application of the imiquimod on days 1–4, the mice received 1280 J/cm^2 RL once daily. On day 5, the mice were sacrificed, and tissue samples were collected for pathological analysis. A vehicle control received petrolatum on days 1–4 and was sacrificed on day 5.

Mouse irradiation

Mice were irradiated daily with RL phototherapy (633 ± 15 nm, Omnilux Revive 2) at a power density of 87 mW/cm^2. Mice were irradiated in temperature-controlled cages to minimize overheating and photothermal effects from the RL array, as previously published. Daily treatment regimens were 640 J/cm^2 twice daily and 1280 J/cm^2 once daily, corresponding to 2 hours twice daily and 4 h once daily, respectively. The ambient temperature was monitored with a temperature probe. Mouse core body temperature was maintained between 34.5 and 38.9 °C, measured using a rectal temperature probe.

Tissue histology

After euthanasia, skin samples were collected and preserved in 10% formalin. These fixed tissues were then submitted to Histowiz (Brooklyn, NY) for processing using their standardized protocol and fully automated workflow, as previously described[20].

Measurement of mouse epidermal thickness and dyskeratosis

Measurements were performed using a single-blinded protocol. Ten images from each tissue sample were selected for analysis by an author (MC). A second blinded measuring author (AK) measured the epidermal thickness at 5 locations within each image. Images were uploaded to ImageJ software and epidermal thickness was measured using the line tool. The measuring author was instructed to draw a perpendicular line from the epidermal-dermal junction to the base of the stratum corneum. The measuring author avoided irregular regions, including tissue damaged in processing, folds, and hair follicles. The length units were converted to μm using the image scale. The 50 measurements from each sample were averaged to yield the epidermal thickness. The slides were visually inspected for dyskeratotic keratinocytes in the epidermis[30]. No statistics were utilized as there was negligible dyskeratosis in any sample.

Statistical analysis

Prism v6.0 software (GraphPad) was used to generate graphs and perform statistical testing. LED-RL treated groups were compared to a temperature-matched control group that was exposed to the same environmental conditions as the treated groups. The treated group ratios were determined by dividing temperature-matched control groups by their matching treated group. Control group ratios were determined by dividing temperature-matched control groups to the monotherapy efficacy of RL at defined fluences and wavelengths, providing clear mechanistic insights into RL-mediated effects and improvements in cellular and murine models of psoriasis. For comparisons between two groups (RL vs. Control), a two-tailed t-test was applied. Experiments involving more than two groups were evaluated using Analysis of Variance (ANOVA), followed by Dunnett's multiple comparison test to assess significance across three groups. A p-value < 0.05 was considered statistically significant. Statistical analyses were performed using GraphPad software, which was also used to generate figures.

Data availability

All data are available in the main text or the supplementary materials.

Received: 7 July 2025; Accepted: 3 November 2025
Published online: 05 December 2025

References

1. Armstrong, A. W. et al. Psoriasis prevalence in adults in the united States. *JAMA Dermatol.* **157**, 940–946 (2021).
2. Vanderpuye-Orgle, J. et al. Evaluating the economic burden of psoriasis in the united States. *J. Am. Acad. Dermatol.* **72**, 961–967e965 (2015).
3. Grozdev, I. et al. Physical and mental impact of psoriasis severity as measured by the compact short Form-12 health survey (SF-12) quality of life tool. *J. Invest. Dermatol.* **132**, 1111–1116 (2012).
4. Lowes, M. A., Suárez-Fariñas, M. & Krueger, J. G. Immunology of psoriasis. *Annu. Rev. Immunol.* **32**, 227–255 (2014).
5. Lewis, D. A., Travers, J. B., Somani, A. K. & Spandau, D. F. The IGF-1/IGF-1R signaling axis in the skin: a new role for the dermis in aging-associated skin cancer. *Oncogene* **29**, 1475–1485 (2010).
6. Travers, J. B. et al. Fibroblast senescence and squamous cell carcinoma: how wounding therapies could be protective. *Dermatol. Surg.* **39**, 967–973 (2013).
7. Boswell, K. et al. Narrowband ultraviolet B treatment for psoriasis is highly economical and causes significant savings in cost for topical treatments. *Br. J. Dermatol.* **179**, 1148–1156 (2018).
8. Slominski, A. T., Zmijewski, M. A., Plonka, P. M., Szaflarski, J. P. & Paus, R. How UV light touches the brain and endocrine system through Skin, and why. *Endocrinology* **159**, 1992–2007 (2018).
9. Slominski, R. M., Chen, J. Y., Raman, C. & Slominski, A. T. Photo-neuro-immuno-endocrinology: how the ultraviolet radiation regulates the body, brain, and immune system. *Proc. Natl. Acad. Sci. U S A.* **121**, e2308374121 (2024).
10. Slominski, R. M., Raman, C., Jetten, A. M. & Slominski, A. T. Neuro–immuno–endocrinology of the skin: how environment regulates body homeostasis. *Nat. Reviews Endocrinol.* **21**, 495–509 (2025).
11. Kleinpenning, M. M., Otero, M. E., van Erp, P. E., Gerritsen, M. J. & van de Kerkhof, P. C. Efficacy of blue light vs. red light in the treatment of psoriasis: a double-blind, randomized comparative study. *J. Eur. Acad. Dermatol. Venereol.* **26**, 219–225 (2012).
12. Hartmann Schatloff, D., Retamal Altbir, C. & Valenzuela, F. The role of excimer light in dermatology: a review. *An. Bras. Dermatol.* **99**, 887–894 (2024).
13. Yoo, J. A. et al. Blue Light Irradiation Induces Human Keratinocyte Cell Damage via Transient Receptor Potential Vanilloid 1 (TRPV1) Regulation. *Oxid. Med. Cell Longev.* **2020**, 8871745 (2020).
14. Liebmann, J., Born, M. & Kolb-Bachofen, V. Blue-light irradiation regulates proliferation and differentiation in human skin cells. *J. Invest. Dermatol.* **130**, 259–269 (2010).
15. Ablon, G. Combination 830-nm and 633-nm light-emitting diode phototherapy shows promise in the treatment of recalcitrant psoriasis: preliminary findings. *Photomed. Laser Surg.* **28**, 141–146 (2010).
16. Niu, T., Tian, Y., Cai, Q., Ren, Q. & Wei, L. Red light combined with blue light irradiation regulates proliferation and apoptosis in skin keratinocytes in combination with low concentrations of Curcumin. *PLoS One*. **10**, e0138754 (2015).
17. Jalal Maghfour, M. *MS, Et al. Photobiomodulation CME Part I: Overview and Mechanism of Action* (Journal of the American Academy of Dermatology, 2024).
18. Lev-Tov, H., Mamalis, A., Brody, N., Siegel, D. & Jagdeo, J. Inhibition of fibroblast proliferation in vitro using red light-emitting diodes. *Dermatol. Surg.* **39**, 1167–1170 (2013).
19. Mamalis, A. et al. High fluence light emitting diode-generated red light modulates characteristics associated with skin fibrosis. *J. Biophotonics*. **9**, 1167–1179 (2016).
20. Austin, E. et al. Red light phototherapy using light-Emitting diodes inhibits melanoma proliferation and alters tumor microenvironments. *Front. Oncol.* **12**, 928484 (2022).
21. Cordoro, K. M. et al. Skin-infiltrating, interleukin-22-producing T cells differentiate pediatric psoriasis from adult psoriasis. *J. Am. Acad. Dermatol.* **77**, 417–424 (2017).
22. Ma, H. L. et al. IL-22 is required for Th17 cell-mediated pathology in a mouse model of psoriasis-like skin inflammation. *J. Clin. Invest.* **118**, 597–607 (2008).
23. Masub, N., Austin, E., Huang, A. & Jagdeo, J. High-fluence light emitting diode-red light inhibits cell cycle progression in human dermal fibroblasts. *J. Biophotonics*. **14**, e202000359 (2021).
24. Sano, S. et al. Stat3 links activated keratinocytes and immunocytes required for development of psoriasis in a novel Transgenic mouse model. *Nat. Med.* **11**, 43–49 (2005).
25. Lian, P. et al. S1PR3-driven positive feedback loop sustains STAT3 activation and keratinocyte hyperproliferation in psoriasis. *Cell. Death Dis.* **16**, 31 (2025).
26. Calautti, E., Avalle, L., Poli, V. & Psoriasis A STAT3-Centric view. *Int J. Mol. Sci* **19**, 1–14 (2018).
27. Wang, J. Y., Austin, E. & Jagdeo, J. Visible red light does not induce DNA damage in human dermal fibroblasts. *J. Biophotonics*. **15**, e202200023 (2022).
28. Jagdeo, J. et al. Safety of light emitting diode-red light on human skin: two randomized controlled trials. *J. Biophotonics*. **13**, e201960014 (2020).
29. Austin, E. et al. Transcriptome analysis of human dermal fibroblasts following red light phototherapy. *Sci. Rep.* **11**, 7315 (2021).
30. Ortner, D. et al. Langerhans cells orchestrate apoptosis of DNA-damaged keratinocytes upon high-dose UVB skin exposure. *Eur. J. Immunol.* **54**, e2451020 (2024).

Author contributions

EA, EK, and JJ conceptualized the study and developed its methodology. EA and EK conducted the experiments. EA, EK, MK, and JJ performed data analysis. EM and RI provided essential equipment. EA, EK, MK, AM, EM, RI, and JJ reviewed the data. JJ acquired funding and supervised the study. EA, EK, and MK wrote the original manuscript draft, while EA, MK, RI, MC, AK, AM and JJ reviewed and edited the manuscript. All authors reviewed and approved the final manuscript.

Funding

This study received no external funding.

Declarations

Competing interests

JJ is on the scientific advisory board of Globalmed Technologies.

Additional information

Supplementary Information The online version contains supplementary material available at https://doi.org/10.1038/s41598-025-27186-4.

Correspondence and requests for materials should be addressed to J.J.

Reprints and permissions information is available at www.nature.com/reprints.

Publisher's note Springer Nature remains neutral with regard to jurisdictional claims in published maps and institutional affiliations.